Angular dependence of the upper critical field in CaAlSi single crystal: Deviation from the Ginzburg-Landau anisotropic mass model

Ajay Kumar Ghosh,* M. Tokunaga, and T. Tamegai[†]
Department of Applied Physics, The University of Tokyo, 7-3-1 Hongo, Bunkyo-ku, Tokyo 113-8656, Japan

The anisotropic upper critical field in CaAlSi with an AlB_2 structure has been investigated by magnetic, transport, and specific heat measurements. The variation of H_{c2} with θ, the angle between the ab plane and the applied field, determined from the transport measurements at various temperatures, show a cusplike behavior near $\theta = 0°$ unlike the prediction of the Ginzburg-Landau anisotropic mass model. Rather, the angular dependence is consistent with Tinkham's formula for thin film superconductors. We have found an increase in the anisotropy parameter with temperature. The negligible in-plane anisotropy of H_{c2} is consistent with the small mean free path in this compound.

The discovery of MgB_2 with an AlB_2 structure has created tremendous interest in investigating the various physical properties of compounds having similar structures.[1] Silicides with AlB_2-structures have been reported recently.[2] Studies of superconducting properties in such systems will be helpful to explain the mechanism of superconductivity in this class of hexagonal materials. Also, the study of these superconductors is related to the technological application of them in devices. Among the various silicides with an AlB_2-type structure is a high pressure superconducting phase of $CaSi_2$ with a T_c of 14 K.[3] Recently, ternary silicides like $Sr(Ga_{0.37}Si_{0.63})_2$ and CaAlSi were reported to be superconducting.[2,4] The common feature of these two silicides is the existence of hexagonal honeycomb layers with randomly distributed Si and Ga or Al and intercalated layers of Sr or Ca. On the basis of a band structure calculation of $CaSi_2$ the electronic structure near the Fermi level was attributed to the mixed state of Sr $4d$ states and p states of Si and Ga in $Sr(Ga_{0.37}Si_{0.63})_2$.[4] According to the band structure calculations, the hybridized states of Ca $3d$ and p states of Al and Si control the superconductivity in CaAlSi.[5] The physical properties are affected both by atoms in (Al, Si) sites as well as Ca sites of the silicide compounds. Some other binary and pseudobinary intermetallic compounds with similar structures are also reported to be superconducting.[6]

In order to investigate the role of honeycomb layers with other intercalated layers anisotropic normal as well as superconducting state properties need to be studied intensively using single crystals. The upper critical field characterizing the normal to superconducting state transition is one such property. Investigating the angular dependence of H_{c2} the roles of various layers and the interaction among them can be explored. We have measured the anisotropic magnetization and transport properties of single crystalline superconducting CaAlSi. The upper critical field has been determined at various angles, θ, from a variation of the resistivity with magnetic field at several temperatures. The variation of the anisotropy parameter with temperature has also been investigated. Results are compared with the existing theories expressing the angular variation of the upper critical field.

The ingots of CaAlSi are prepared by arc melting a 1:1:1 stoichiometric mixture of Ca, Al, and Si in an Ar environ-ment. The ingots are then used to prepare the feeding and seed rods for the floating-zone method to grow the single crystal. Single crystals are grown with a growth rate of 2 mm/h in an Ar environment with a flow rate of 1 l/min. The rods are rotated in the opposite directions at an angular speed of 20 rpm. Single crystals with shiny surfaces are extracted for the measurements. The typical dimensions of the crystals are $3.0 \times 1.0 \times 1.0$ mm^3. The magnetization measurements as a function of temperature are done with applied field both parallel and perpendicular to the c axis using a superconducting quantum interference device magnetometer (MPMS-XL, Quantum Design). The transport measurements are done using a four-probe method. We have measured the resistivities along the c axis and ab plane as a function of temperature by putting different contacts for the two cases so that the current flows uniformly. The in-plane resistivity is measured as a function of the magnetic field at various temperatures. A vector magnet system with horizontal and vertical components and a two-axis sample rotator is used to apply the magnetic field in any direction. We have also measured the resistivity as a function of the magnetic field for various in-plane angles. The specific heat as a function of the temperature has been measured at several fields for $H \| ab$ by the relaxation method.

The critical temperature of single crystalline CaAlSi is determined from field-cooled and zero field-cooled magnetizations at 5 Oe, shown in the inset of Fig. 1(a). The onset critical temperature is 6.0 K, with a transition width of 0.2 K, as shown in the inset of Fig. 1(a). The resistivity along the c axis and ab plane is shown in the inset of Fig. 1(b). The ratio of ρ_c / ρ_{ab} is about 3.1 at room temperature. The field-cooled magnetization (M) at various magnetic fields for $H \| c$ and $H \| ab$ is shown in Fig. 1. The upper critical fields H_{c2}^c and H_{c2}^{ab} are determined from the onset of diamagnetism as shown in Fig. 1(a). The variations of H_{c2}^c and H_{c2}^{ab} are plotted in Fig. 2. The anisotropic nature of CaAlSi sample is revealed clearly. On close inspection it is revealed that though the variation of H_{c2}^c is linear below 5.5 K that of H_{c2}^{ab} is not, particularly below 4.5 K. We have also shown H_{c2} in Fig. 2 obtained from the specific heat measurements (see the inset
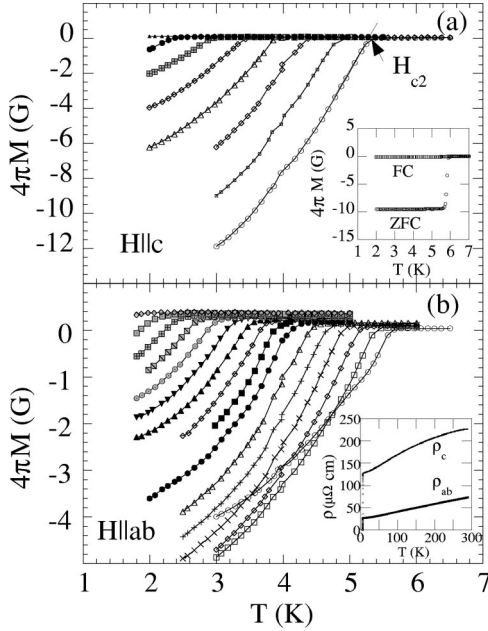
FIG. 1. Field-cooled magnetization as a function of the temperature. (a) is for $H||c$ from 1 to 8 kOe, and (b) is for $H||ab$ from 1 kOe to 16 kOe with intervals of 1 kOe. The inset of (a) shows the temperature dependence of the field-cooled (FC) and zero field-cooled magnetizations at 5 Oe. The inset of (b) shows the variation of resistivities along the c axis (ρ_c) and the ab plane (ρ_{ab}).

of Fig. 2) at several magnetic fields for $H||ab$, which clearly supports the bulk nature of superconductivity in CaAlSi for this configuration.

For dirty isotropic s-wave superconductors, the extrapolated upper critical field is given by $H_{c2}(0) = -0.69 T_c(\partial H_{c2}/\partial T)$. The slopes of $H_{c2}^{ab}(T)$ and $H_{c2}^c(T)$ are -4.05 and -2.08 kOe/K, respectively. The related values are $H_{c2}^{ab}(0) \sim 16.8$ kOe and $H_{c2}^c(0) \sim 8.6$ kOe which are equivalent to an anisotropy of 1.95. We have extracted the coherence lengths $\xi_c(0)$ and $\xi_{ab}(0)$ from the relations $\xi_{ab}(0) = [\Phi_0/2\pi H_{c2}^c(0)]^{1/2}$ and $\xi_c(0) = \Phi_0/2\pi H_{c2}^{ab}(0)\xi_{ab}(0)$, where Φ_0 is the flux quantum. From the above critical field values, the coherence lengths
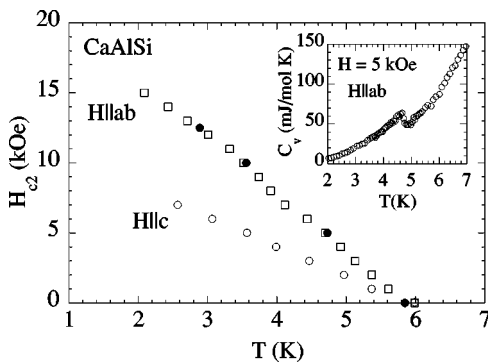
FIG. 2. The upper critical fields of CaAlSi for $H||c$ (open circle) and $H||ab$ (open square) extracted from $M-T$ and specific heat (solid circle) measurements. The inset shows the specific heat as a function of temperature at 5 kOe for $H||ab$.
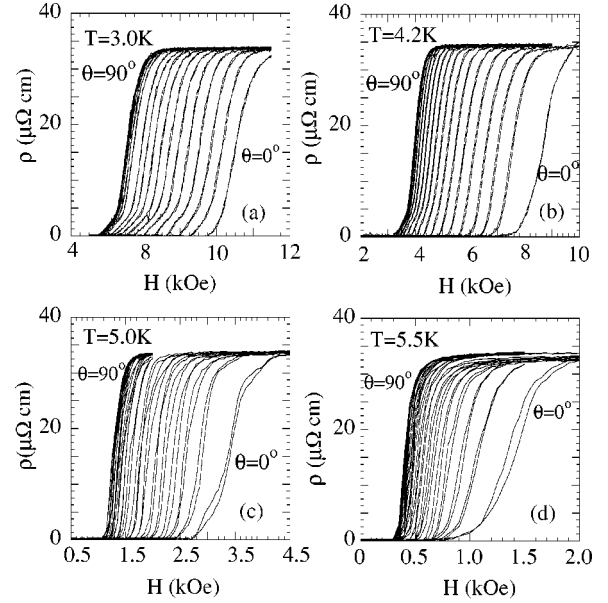
FIG. 3. The resistivity as a function of applied magnetic field at various angles from $\theta = 0°$ to $\theta = 90°$ every 5° at (a) $T = 3.0$ K, (b) 4.2 K, (c) 5.0 K, and (d) 5.5 K. The two lines for each angle are for increasing and decreasing magnetic fields.

are calculated as $\xi_{ab}(0) = 196$ Å and $\xi_c(0) = 100$ Å . The mean free path is calculated from $l = 3/[\rho N(0) v_F e^2]$ [ρ is the resistivity, $N(0)$ the density of states at Fermi level, v_F the Fermi velocity]. According to the band structure calculation of CaAlSi, the density of states (DOS) at the Fermi level is contributed by Ca$-3d$ states which dominate over the $3p$ states of Al and Si (about six times). The total DOS at the Fermi level [$N(0)$, 1/eV/cell] is 1.13.[5] Since no measurements have been reported on v_F for CaAlSi, we assume the values for MgB$_2$ to obtain a rough estimation.[7] l is estimated as 29 Å in CaAlSi, from which we confirm our assumption $l \ll \xi$ that CaAlSi belongs to dirty superconductors.

The resistivity as a function of the applied magnetic field (H) is shown in Fig. 3 for four temperatures: 3.0, 4.2, 5.0, and 5.5 K. Each panel of Fig. 3 is for angles θ ranging from 0° to 90° with an interval of 5°. We have also measured negative θ and close to $\theta = 0°$ with closely spaced intervals. The upper critical field H_{c2} has been determined from the criterion of $\rho = 0.5\rho_n$, where ρ_n is the normal state resistivity. In Fig. 4, H_{c2} is plotted as a function of θ. It is observed that there is a cusplike behavior close to $\theta = 0°$. This feature is found at all measured temperatures as revealed in Fig. 4. In addition, we have extracted H_{c2} with the conditions $\rho = 0.1\rho_n$ and $\rho = 0.9\rho_n$ which show similar cusplike variations with θ as shown in the inset of Fig. 4.

According to the Ginzburg-Landau (GL) anisotropic mass model the variation of H_{c2} can be represented as[8]

$$H_{c2}(\theta) = H_{c2}^{||}(\cos^2\theta + \gamma^2\sin^2\theta)^{-0.5}. \quad (1)$$

Here, $H_{c2}^{||}$ is the critical field corresponding to $\theta = 0°$ and γ is the anisotropy parameter. We have plotted the $H_{c2}(\theta)$ from Eq. (1) in Fig. 4 with the dotted lines. The experimental data points clearly deviate from this behavior, particularly
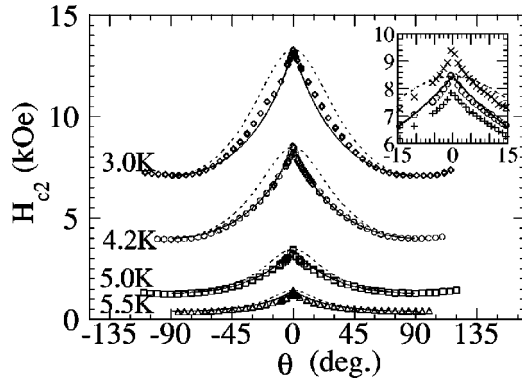
FIG. 4. The variations of the upper critical field with the angle θ for the temperatures 3.0, 4.2, 5.0, and 5.5 K. The solid and dotted lines are Tinkham's formula and the GL model, respectively. The inset shows the magnified cusp region at 4.2 K which is well reproduced by Tinkham's formula. H_{c2}, with the conditions $\rho = 0.1 \rho_n$ and $\rho = 0.9 \rho_n$ at 4.2 K, are shown in the inset by cross and plus symbols, respectively.

around $\theta = 0°$. In the case of MgB$_2$, it is found that the GL model can well describe the angular variation of H_{c2} measured by the torque magnetometry.[9]

Starting from the GL equation and based on the flux quantization, Tinkham calculated the variation of $H_{c2}(\theta)$ for a thin film of thickness d satisfying the condition $d \ll \xi$. The formulation shows that the angular dependence can be expressed as[10]

$$\left| \frac{H_{c2}(\theta)\sin\theta}{H_{c2}^{\perp}} \right| + \left(\frac{H_{c2}(\theta)\cos\theta}{H_{c2}^{\parallel}} \right)^2 = 1. \qquad (2)$$

In this case, $H_{c2}^{\perp}$ and $H_{c2}^{\parallel}$ are the critical fields for $\theta = 90°$ and $\theta = 0°$, respectively. We have found that Eq. (2) nicely reproduces the experimental data points (see Fig. 4). In the region of small θ, the cusplike behavior of Tinkham's formula matches well with the experimental H_{c2} values, as shown in the inset of Fig. 4 for 4.2 K. However, since we are dealing with a bulk single crystal with its thickness much larger than ξ_c, application of the thin film formula seems unreasonable.

In superconducting multilayers formed by artificial deposition of superconducting and nonsuperconducting layers there have been several reports on the crossover from a GL-like three-dimensional (3D) character to a Tinkham-like 2D character induced by the temperature or thickness of nonsuperconducting layers.[11] In these reports the coupling between the superconducting layers is caused either by Josephson tunneling or by proximity effects in the presence of insulating layers (Nb/Ge)(Ref. 12) or normal layers (Nb/Cu),[13] respectively. In Nb/Cu multilayers, the angular dependence of H_{c2} shows a transformation from a rounded behavior to a cusplike behavior continuously induced by the change in d_{Cu}, the thickness of the Cu layer, from $\xi_c = d_{Cu}$ to $\xi_c = 6d_{Cu}$. Tinkham's formula predicts that the slope around $\theta \to 0°$ should be expressed by, $|dH_{c2}/d\theta| = (H_{c2}^{\parallel})^2/2H_{c2}^{\perp}$, while it approaches zero in the GL model. On a close inspection of $H_{c2}(\theta)$, the best fitting to Tinkham's formula is found
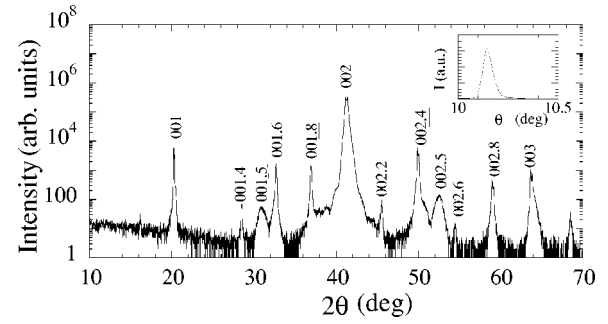
FIG. 5. X-ray diffraction pattern in the $\theta - 2\theta$ scan showing (00l) peaks. The inset shows the θ scan for the (001) peak.

for 4.2 K. However, at intermediate angles the deviation between the experimental points and the theoretical formula is evident as in the cases of 3.0 and 5.5 K. A similar deviation from Tinkham's formula in the two-dimensional regime is observed in Nb/Cu.[13] It should be noted that a cusplike behavior occurs even in multilayers with a relatively small anisotropy. In Nb/Cu multilayers, the slope $1/H_{c2}(dH_{c2}/d\theta)$ is almost zero only when $H_{c2}^{ab}/H_{c2}^{c} \lesssim 1.5$. As soon as $H_{c2}^{ab}/H_{c2}^{c} > 2$, the slope becomes finite, indicating the presence of two-dimensional superconductivity.[13]

In the case of multilayers, the two dimensionality is expected in the condition $d_n > \xi_c > d_s$, where d_n and d_s are the thicknesses of the normal and superconducting layers. This means that the presence of a rather thick normal layer is required for the presence of cusplike behavior. In order to pursue such a possibility, we reexamine the structure of CaAlSi. In Fig. 5, we show an x-ray diffraction pattern in the $\theta - 2\theta$ scan. Here we set the crystal on a diffractometer so that the c-axis is perpendicular to the x ray for $2\theta = 0°$. Clear fivefold and twofold superstructure peaks are observed, from which the real c-axis lattice constant is 21 Å for the former case. How these two kinds of superstructures (co)exist is not clear. Furthermore, the origin of superstructures and which layer is superconducting is a matter of future study. Despite all these uncertainties, the larger c-axis unit cell opens a possibility for the thick normal layer separating superconducting layers in CaAlSi. Admittedly the presence of a superstructure certainly helps to make the system more two dimensional; still the condition $d_n > \xi_c (= 100 \text{ Å})$ is not satisfied. Whether a two-dimensional behavior is possible when d_n is comparable to or slightly smaller than ξ_c should be clarified in due course. Alternatively, CaAlSi may have additional inhomogeneities of a much larger scale, such as planar inclusions, to make the system more two dimensional. It is interesting to note that the variation of H_{c2} in another hexagonal layered superconductor Cs$_{0.2}$WO$_3$ with the polar angle, θ, shows a similar variation.[14] Also, it is reported that $H_{c2}(\theta)$ in MgB$_2$ single crystal shows deviation from the GL model.[15]

We have extracted the anisotropy parameter $\gamma = H_{c2}^{ab}/H_{c2}^{c}$ from both magnetization and transport measurements, and plotted them in Fig. 6(a) as functions of the reduced temperature $t = T/T_c$. γ in CaAlSi increases with the increase in temperature. This is, to the best of our knowledge, the first experimental observation of the increase in γ with temperature in superconductor with a MgB$_2$-like structure.[16] It is important to mention that the increase in γ with temperature
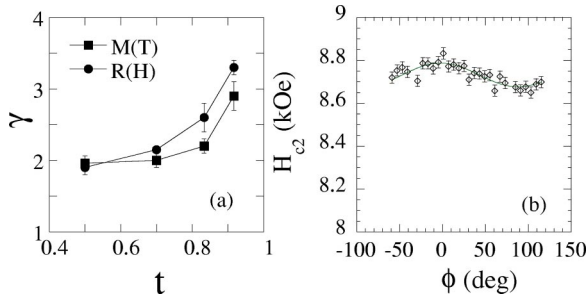
FIG. 6. (a) Anisotropy parameter as a function of the reduced temperature (t) extracted from transport and magnetization measurements. (b) In-plane upper critical fields at various in-plane angles ϕ at 4.2 K. H_{c2} has been determined from the criterion of $\rho = 0.5\rho_n$, where ρ_n is the normal state resistivity. The line is a fit to the data points, $H_{c2}(\phi) = a\,\cos(2\phi) + b$.

has been observed in single crystal of $(LaSe)_{1.14}(NbSe_2)$.[17] γ at 0.1 K is about 40, which increases to 130 at 1 K and decreases to 50 with a further increase in temperature to 1.2 K.[17] Since the detailed structure of the Fermi surface and the order parameter of CaAlSi are not available, we try to compare the present results in terms of the model applicable for MgB_2, the structural analog of CaAlSi. Assuming the anisotropic nature of the order parameter, $\Delta_c > \Delta_{ab}$, the increase in γ with temperature is predicted for MgB_2.[18]

We have also measured the in-plane variation of H_{c2} as a function of the in-plane angle, ϕ, using the resistivity as a function of the magnetic field at 4.2 K. The variation of $H_{c2}(\phi)$ is shown in Fig. 6(b). The angle $\phi = 0°$ represents the direction of the current. The observed twofold symmetry in $H_{c2}(\phi)$ of CaAlSi in Fig. 6(b) is attributed to the effect of Lorentz force. The in-plane anisotropy $H_{c2}^{max}(\phi)/H_{c2}^{min}(\phi)$ is about 1.02 at 4.2 K ($t = 0.7$), including the Lorentz force

effect. The sixfold symmetry component consistent with the crystal symmetry is much smaller than that. It would be interesting to mention that the ratio of $H_{c2}^{max}(\phi)/H_{c2}^{min}(\phi)$ is 1.95 in $Cs_{0.2}WO_3$ with $H_{c2}^{max}(\phi)$ and $H_{c2}^{min}(\phi)$ at $\phi = 60°$ and $\phi = 90°$, respectively. In $Cs_{0.1}WO_{2.9}F_{0.1}$, $H_{c2}^{max}(\phi)/H_{c2}^{min}(\phi)$ is 1.33 at $t = 0.7$. In both cases, $H_{c2}(\phi)$ exhibits a clear sixfold symmetry at $t = 0.8$ which is attributed to the hexagonal crystal symmetry of the superconductors.[14,19] In borocarbide superconductor, the ratio, $H_{c2}^{\langle 100 \rangle}/H_{c2}^{\langle 110 \rangle}$ is found to be 1.03 with a fourfold symmetry.[20] In the present case we have no clear signature of the periodic nature of the in-plane $H_{c2}(\phi)$, which is consistent with the fact that CaAlSi belongs to dirty superconductors where local electrodynamics should apply.

In conclusion, we present measurements of the magnetization with temperature and resistive properties with the magnetic field applied at various angles with respect to the hexagonal plane of single crystalline CaAlSi. The upper critical fields show an anisotropic behavior. The angular variation of the upper critical field obtained from the transport measurements shows a cusplike behavior near $\theta = 0°$ consistent with Tinkham's model for thin films. H_{c2} obtained from specific heat data clearly reveals the absence of surface superconductivity in CaAlSi. The anisotropy parameter in CaAlSi obtained from $\rho(H)$ and $M(T)$ increases with temperature. The ratio of the resistivities along the c axis and ab plane is about 3.1 at ambient temperature. No intrinsic in-plane anisotropy has been observed.

*Permanent Address: Department of Physics, Jadavpur University, Kolkata 700032, India

†Electronic address: tamegai@ap.t.u-tokyo.ac.jp

[1] J. Nagamatsu, N. Nakagawa, T. Muranaka, Y. Zenitani, and J. Akimitsu, Nature (London) **410**, 63 (2001).

[2] M. Imai, E. Abe, J. Ye, K. Nishida, T. Kimura, K. Honma, H. Abe, and H. Kitazawa, Phys. Rev. Lett. **87**, 077003 (2001).

[3] S. Sanfilippo, H. Elsinger, M. N. Regueiro, O. Laborde, S. Le-Floch, M. Affronte, G. L. Olcese, and A. Palenzona, Phys. Rev. B **61**, R3800 (2000).

[4] M. Imai, K. Nishida, T. Kimura, and H. Abe, Appl. Phys. Lett. **80**, 1019 (2002).

[5] I. R. Shein, V. V. Ivanovskaya, N. I. Medvedeva and A. L. Ivanovskii, Pis'ma Zh. Éksp. Teor. Fiz. **76**, 223 (2002) [JETP Lett. **76**, 189 (2002)].

[6] R. L. Meng, B. Lorenz, Y. S. Wang, J. Cmaidalka, Y. Y. Sun, Y. Y. Xue, J. K. Meen, and C. W. Chu, Physica C **382**, 113 (2002); B. Lorenz, J. Lenji, J. Cmaidalka, R. L. Meng, Y. Y. Sun, Y. Y. Xue, and C. W. Chu, *ibid.* **383**, 191 (2002).

[7] A. K. Pradhan, Z. X. Shi, M. Tokunaga, T. Tamegai, Y. Takano, K. Togano, H. Kito, and H. Ihara, Phys. Rev. B **64**, 212509 (2001).

[8] G. Blatter, M. V. Feigel'man, V. B. Geshkenbein, A. I. Larkin, and V. M. Vinokur, Rev. Mod. Phys. **66**, 1325 (1994).

[9] M. Angst, R. Puzniak, A. Wisniewski, J. Jun, S. M. Kazakov, J. Karpinski, J. Roos, and H. Keller, Phys. Rev. Lett. **88**, 167004 (2002).

[10] M. Tinkham, Phys. Rev. **129**, 2413 (1963).

[11] A. Sidorenko, C. Surgers, T. Trappmann, and H. v. Lohneysen, Phys. Rev. B **53**, 11 751 (1996).

[12] S. T. Ruggiero, T. W. Barbee Jr., and M. R. Beasley, Phys. Rev. B **26**, 4894 (1982).

[13] C. S. L. Chun, G. G. Zheng, J. L. Vicent, and I. K. Schuller, Phys. Rev. B **29**, 4915 (1984).

[14] M. R. Skokan, W. G. Moulton, and R. C. Morris, Phys. Rev. B **20**, 3670 (1979).

[15] Y. Eltsev, S. Lee, K. Nakao, N. Chikumoto, S. Tajima, N. Koshizuka, and M. Murakami, Physica C **378-381**, 61 (2002); Z. X. Shi *et al.* (unpublished).

[16] M. Zehetmayer, M. Eisterer, J. Jun, S. M. Kazakov, J. Karpinski, A. Wisniewski, and H. W. Weber, Phys. Rev. B **66**, 052505 (2002).

[17] P. Samuely, P. Szabo, J. Kacmarcik, A. G. M. Jansen, A. Lafond, A. Meerschaut, and A. Briggs, Physica C **369**, 61 (2002).

[18] S. Haas and K. Maki, Phys. Rev. B **65**, 020502(R) (2001).

[19] M. R. Skokan, R. C. Morris, and W. G. Moulton, Phys. Rev. B **13**, 1077 (1976).

[20] V. Metlushko, U. Welp, A. Koshelev, I. Aranson, G. W. Crabtree, and P. C. Canfield, Phys. Rev. Lett. **79**, 1738 (1997).